

A Bio-inspired Gliding-enabled Flapping Wing Aerial Robot Platform: Design, Build, and Characterization

OVERVIEW

Seagulls and albatrosses can glide for extended periods by exploiting wind shear layers near the ocean surface through dynamic soaring, gaining energy without flapping. Inspired by this flight pattern, we propose a bird-scale flapping wing vehicle (BFWV) to serve as an experimental platform for investigating dynamic soaring and advancing the understanding of energy-efficient flight.

HOVERING VS. TRANSLATIONAL FLYERS

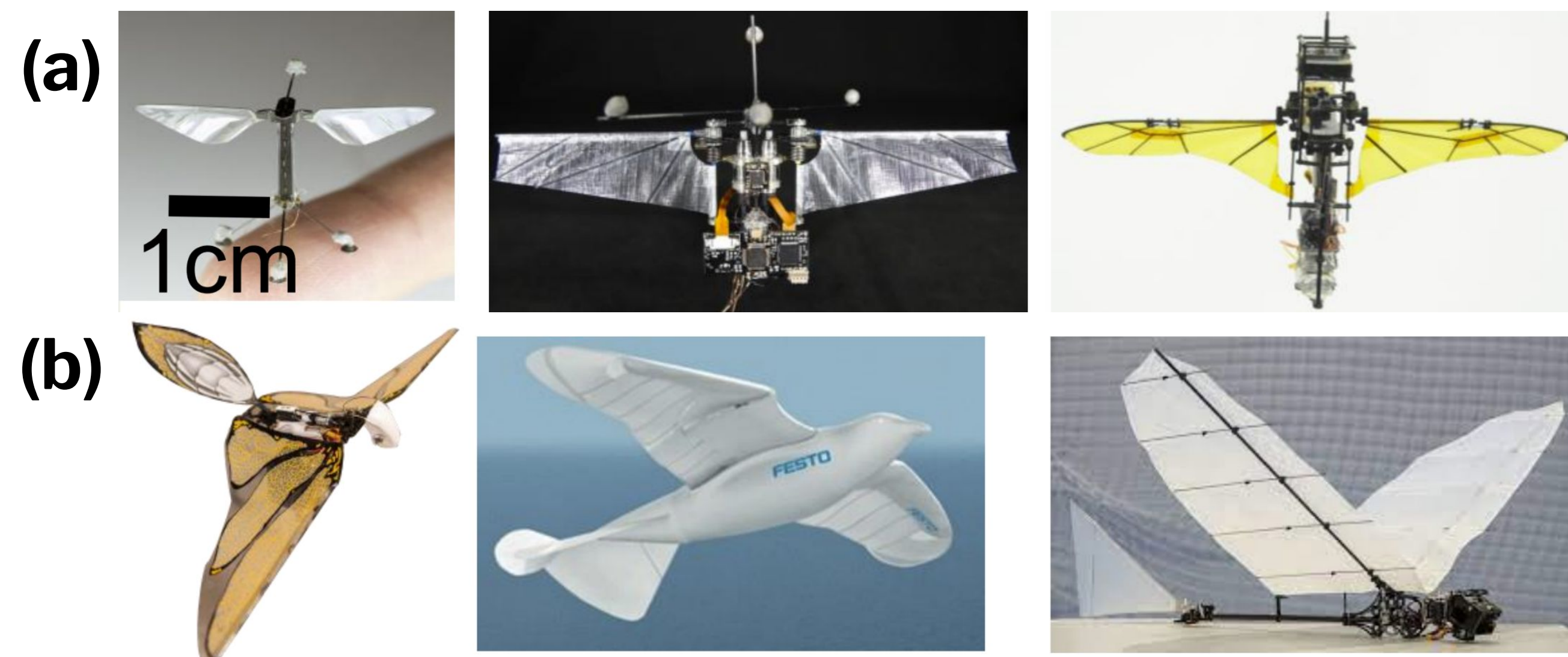


Fig. 1: Hovering flyers (a) generate lift at near-zero forward speed (low-Re), while translational flyers (b) fly with nonzero forward velocity where aerodynamics are dominated by forward motion (high-Re) and efficient lift-drag production.

Rayleigh Cycle

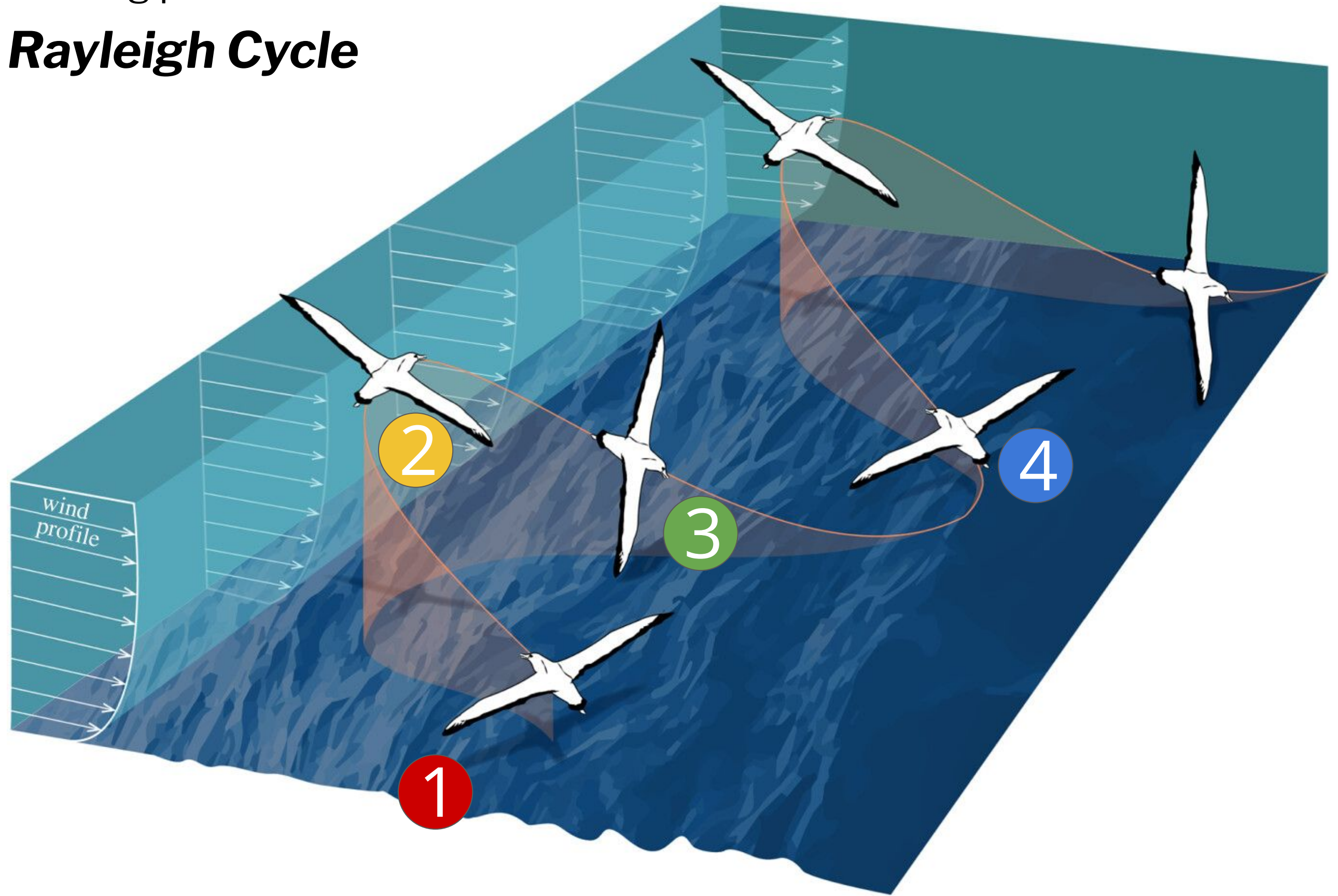


Fig. 2: The Rayleigh cycle is a dynamic soaring loop that harvests energy from a wind-speed gradient. (1) Climb upwind through the shear layer into faster air. (2) Turn at the top to align with the wind. (3) Dive downwind, trading altitude for airspeed back toward low altitude. (4) Turn windward near sea level to repeat the cycle.

Key Design Criteria

- Non-zero freestream velocity (5 – 10 m/s)
- Low flapping frequency (1 – 5 Hz)
- High wing aspect ratio (> 4)
- Large wingspan (>1.0 m)
- Highly cambered wings (8% – 10% of chord)

MECHANICAL DESIGN AND ANALYSIS

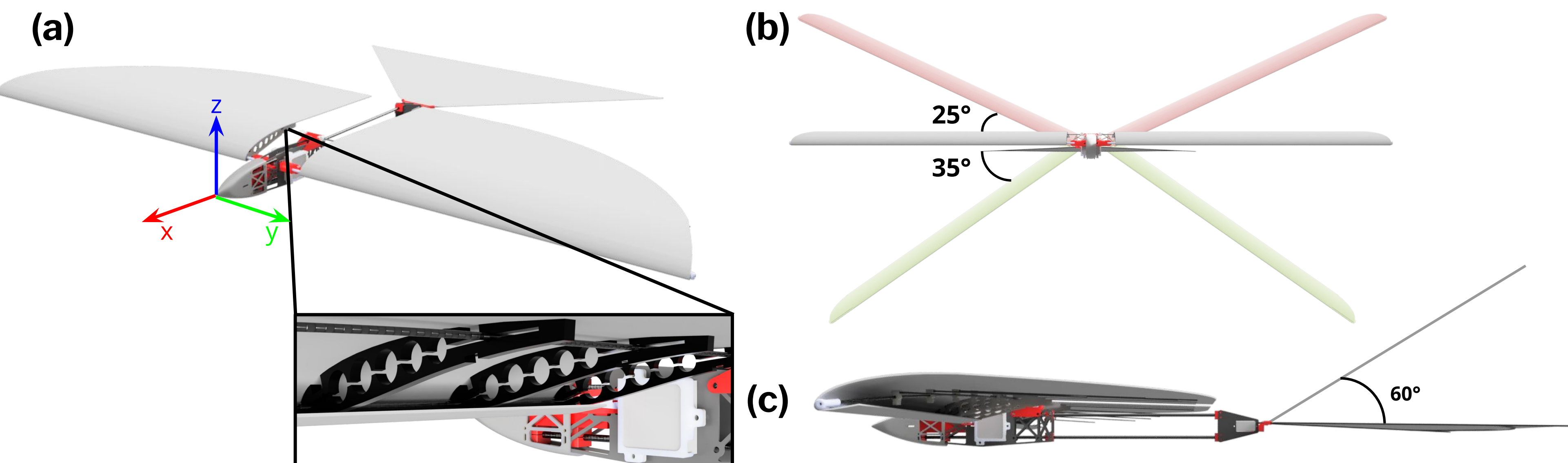


Fig. 3: Computer illustration of the Gliding-Enabled Mode-switching Unmanned Sensing Flapping Wing Vehicle (GEMUS FWV). The mechanical design for the vehicle was done via Onshape, SOLIDWORKS, and Autodesk Inventor. (a) Isometric view of GEMUS with magnified view of wing internals, (b) flapping range of motion during upstroke (red) and downstroke (green), (c) tail range of motion

Computer Aided Engineering (CAE)

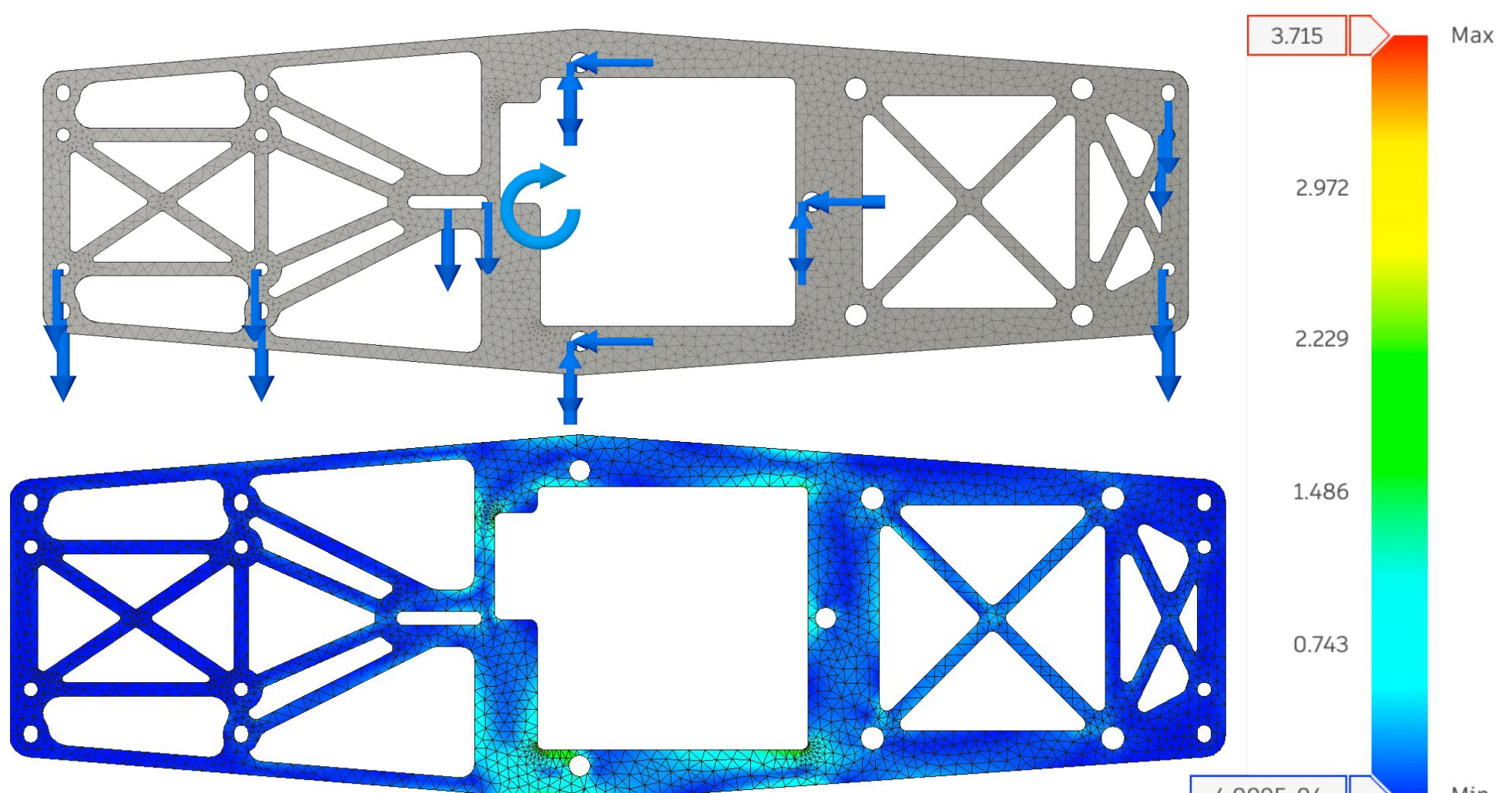


Fig. 4: Von Mises stress distribution from Ansys Mechanical finite element analysis (FEA) of fuselage frame when subject to aerodynamic loads, including lift, drag, tail pitching moment, and servo weight. Minimum safety factor is 222.7 for carbon fiber and 8.3 for PLA.

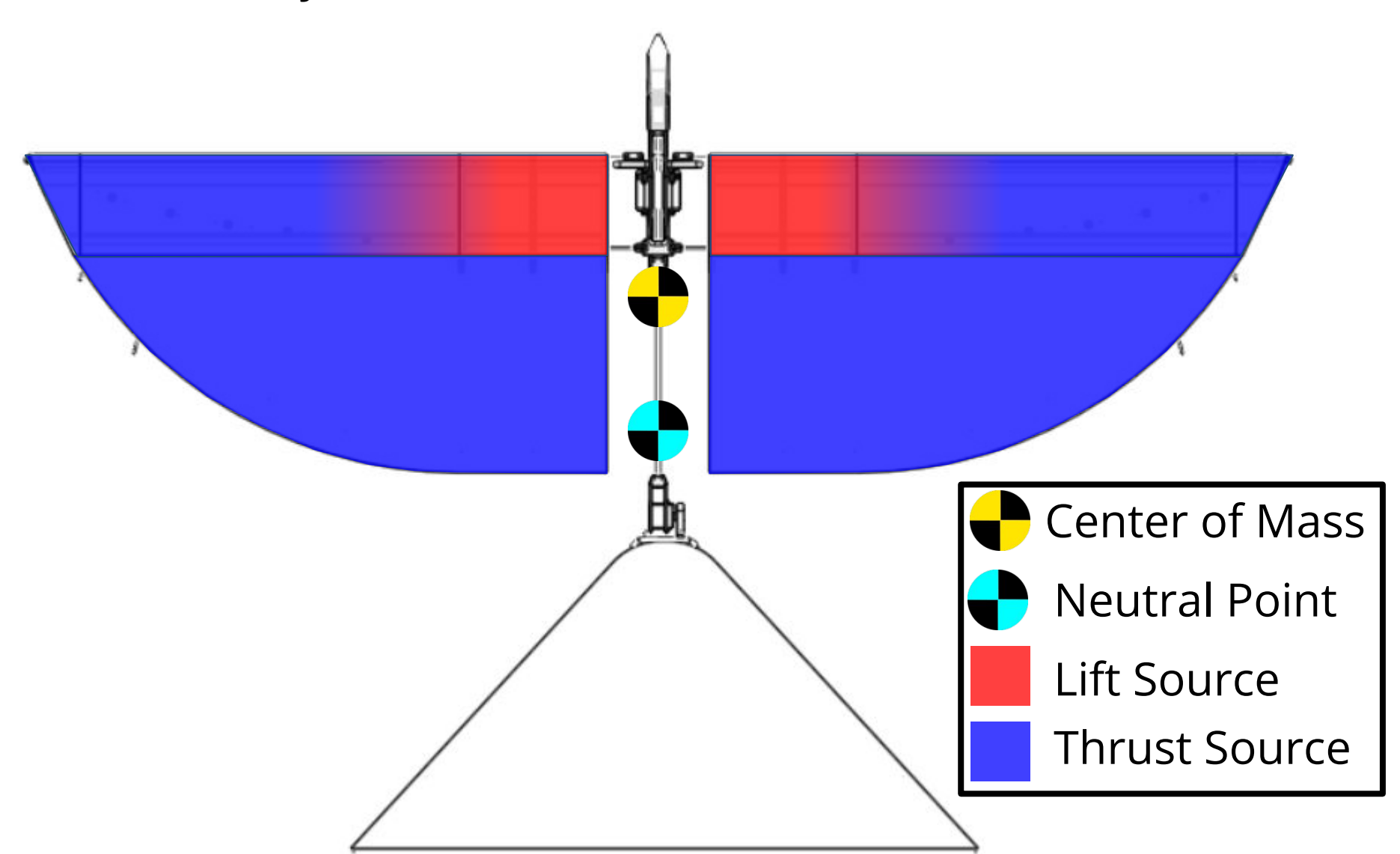


Fig. 6: Vehicle aerodynamic characteristics, including neutral point and center of mass approximation from XFLR5 and estimations of lift/thrust concentrations throughout wing cross-section based on relative torsional stiffness.

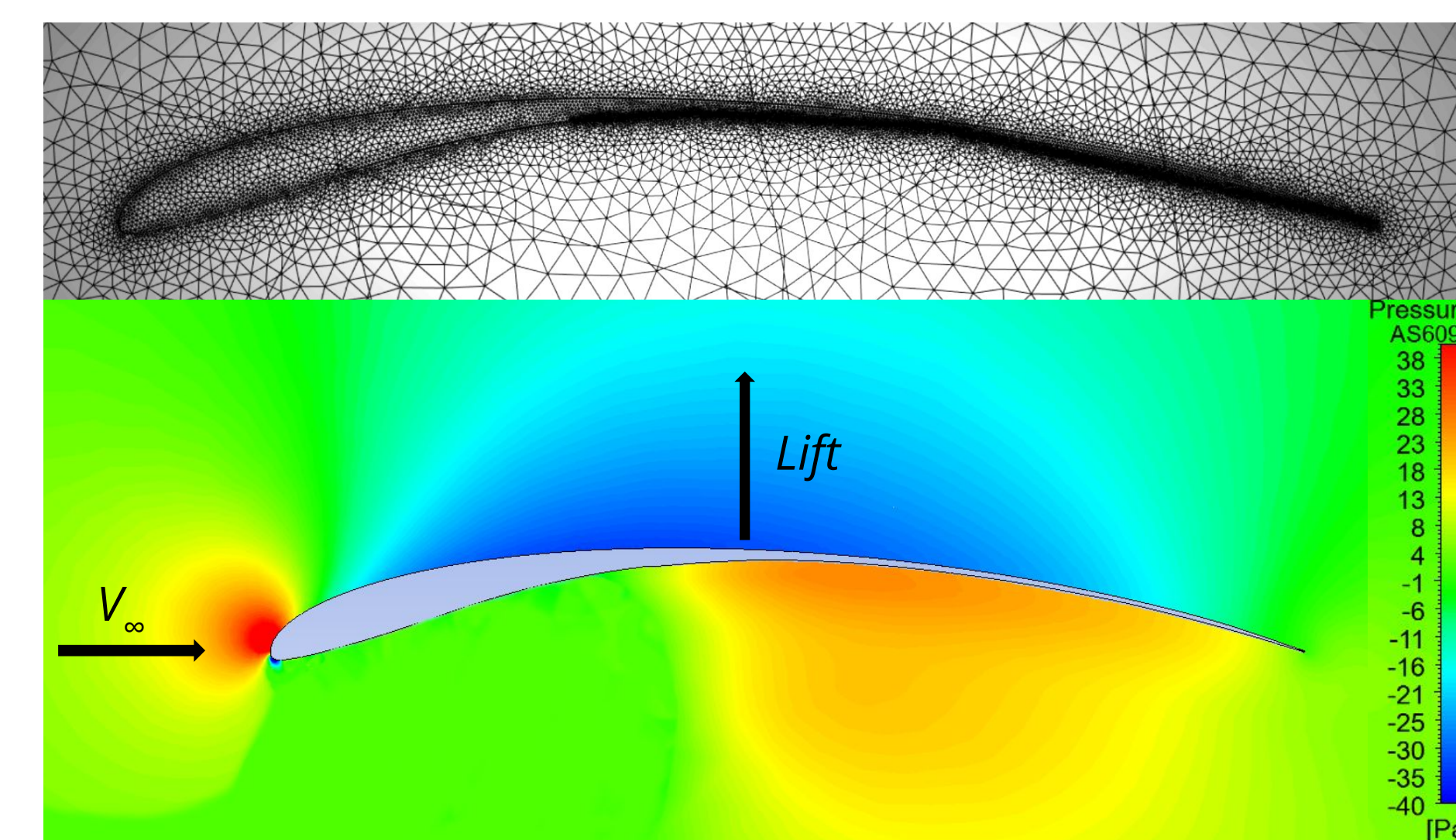
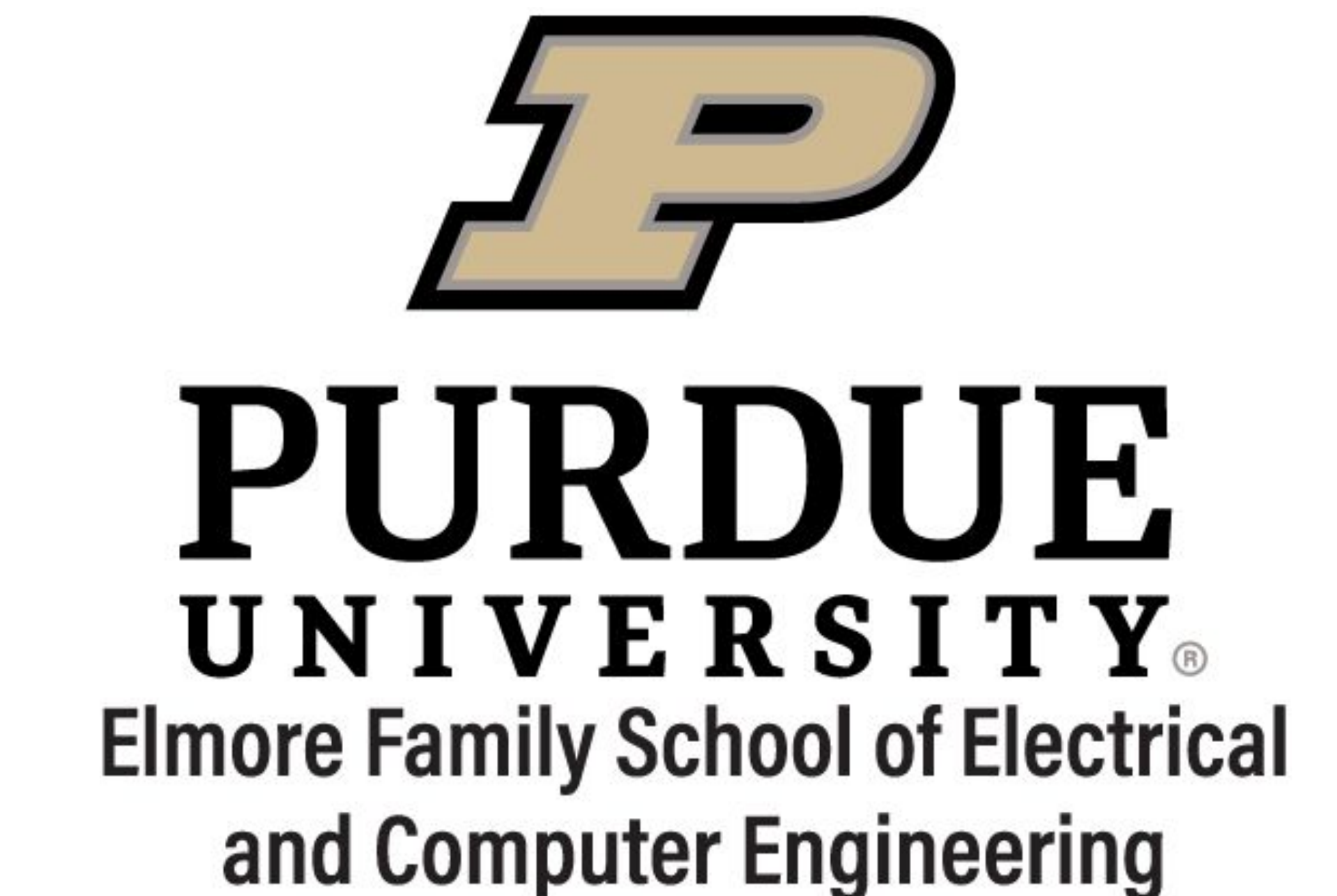


Fig. 5: (a) AS6098 mesh using 186,671 nodes, (b) AS6098 pressure distribution from Ansys Fluent's transient k-omega computational fluid dynamics (CFD) solver. At 0° angle of attack and 10 m/s freestream velocity, the 0.6 m span finite wing is estimated to produce around 4.17 N of lift and 0.53 N of drag.

	GEMUS	Glaucous-Winged Gull
Wingspan (mm)	1215	1200 – 1500
Root Chord (mm)	309.4	392 – 480
Body Length (mm)	794.3	500 – 680
Aspect Ratio	4.41	6.50 – 8.00
Weight (g)	339	730 – 1690
Static Margin	+0.113	

Tab. 1: Key system characteristics of the FWV compared to common glaucous-winged gull



Shijun Zhou¹, Gilbert Chang², Logan Dihel², Jaden Hernandez³, Nak-seung Hyun²

SIMULATION

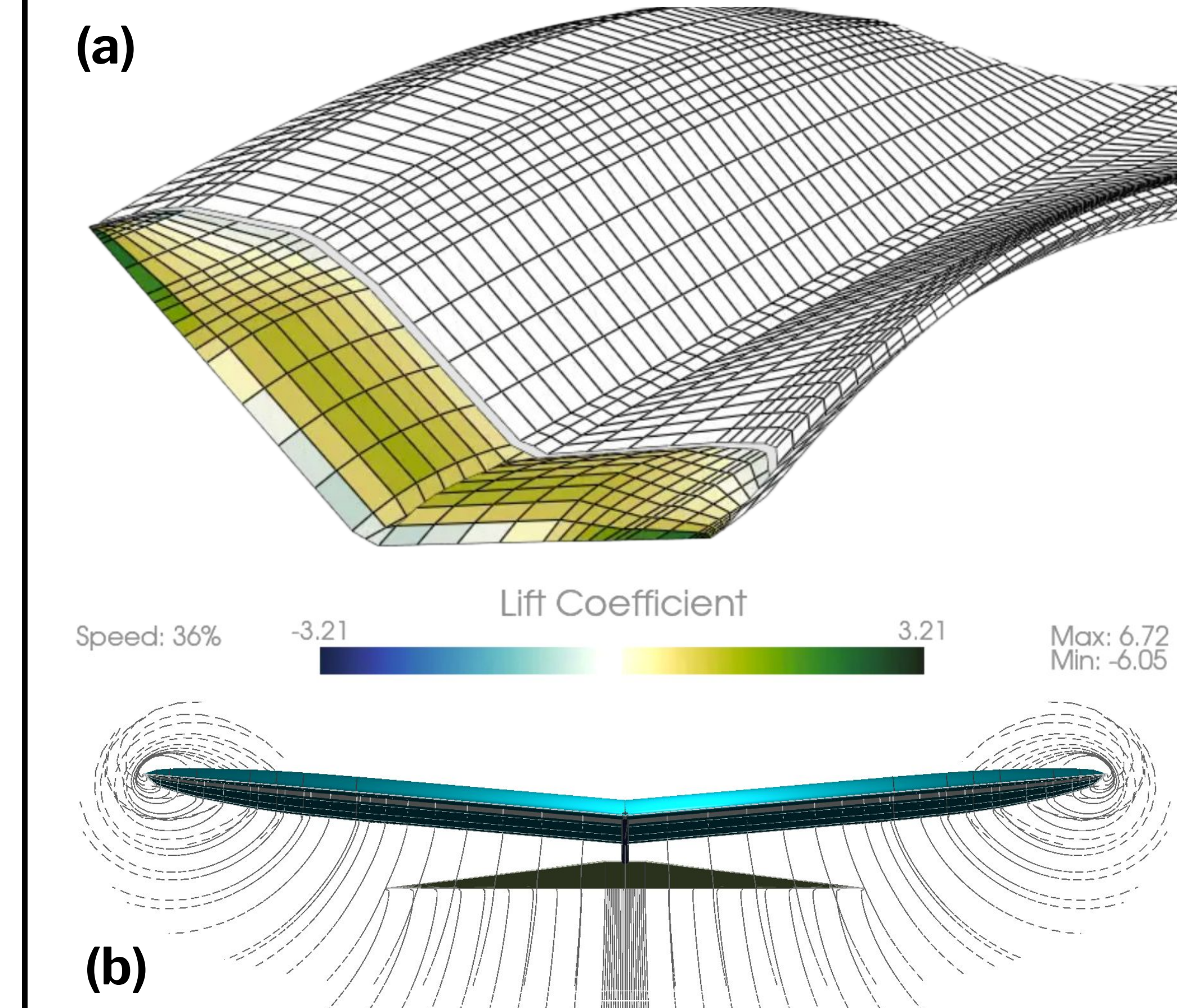


Fig. 7: Vortex lattice method simulation in (a) unsteady, flapping case to verify lift/thrust capabilities for 1 – 5 Hz flapping frequency (Ptera Software) and (b) steady, gliding case to validate longitudinal static stability (XFLR5)

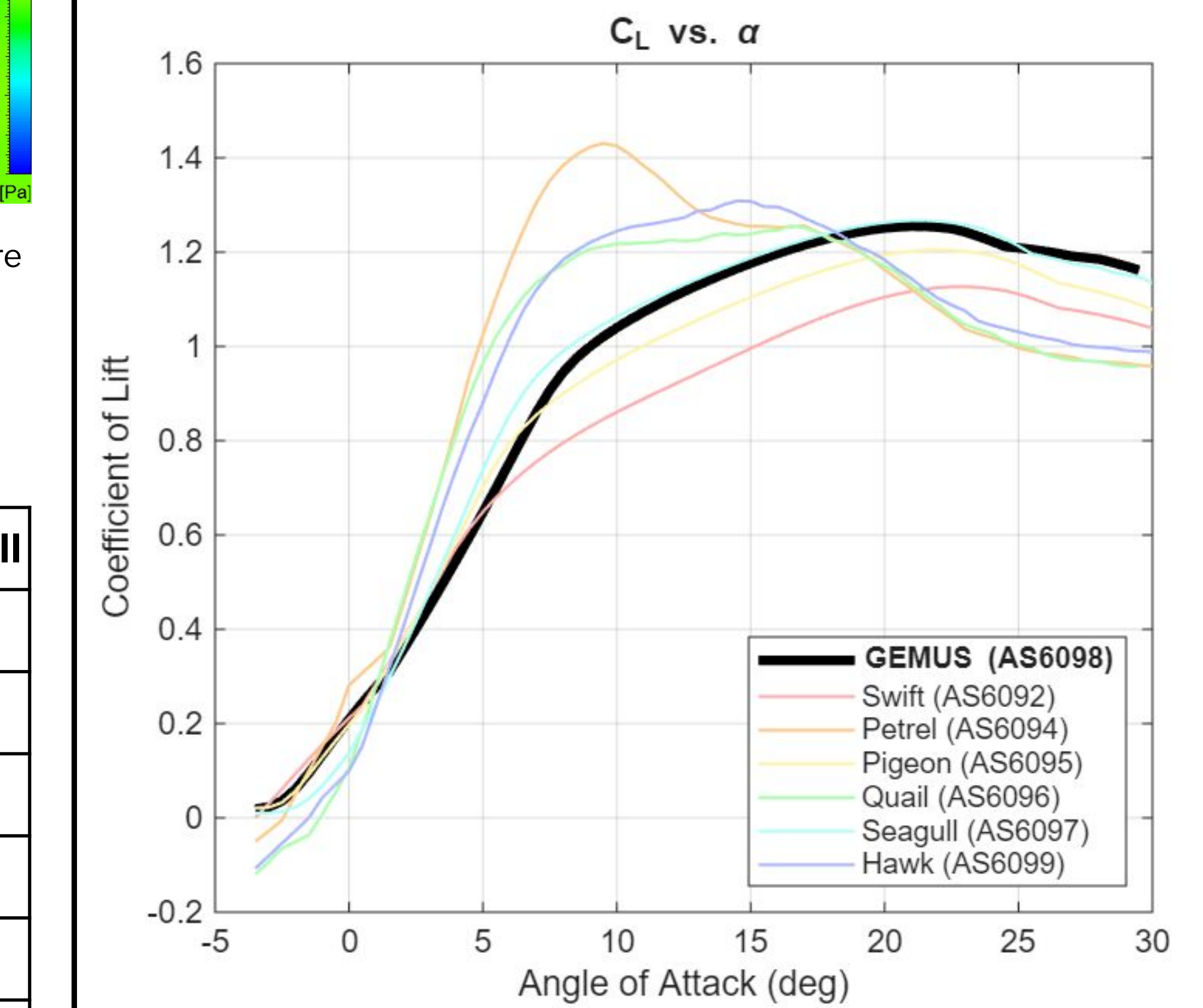


Fig. 8: Airfoil lift performance analysis via panel method for bird-like airfoils from -5° – 30°. (XFLR5)